

Imaging the Finger Force Direction

Yu Sun, John M. Hollerbach
School of Computing
University of Utah
Salt Lake City, UT 84112
{ysun,jmh}@cs.utah.edu

Stephen A. Mascaró
Department of Mechanical Engineering
University of Utah
Salt Lake City, UT 84112
smascaró@mech.utah.edu

Abstract

This paper presents a method of imaging the coloration pattern in the fingernail and surrounding skin to infer fingertip force direction during planar contact. Nail images from 7 subjects were registered to reference images with RANSAC and then warped to an atlas with elastic registration. Recognition of fingertip force direction, based on Linear Discriminant Analysis, shows that there are common color pattern features in the fingernail and surrounding skin for different subjects. Based on the common features, the overall recognition accuracy is 92%.

1. Introduction

Due to the interaction between the fingernail, bone, and tissue, the pools of blood under the fingernail are affected by the pressure at the fingerpad during contact with a surface. The blood pools create color patterns in the nail that provide a transduction of fingerpad shear and normal force [7, 8]. Mascaró and Asada [7] have proposed a *photoplethysmograph sensor*, comprised of an array of 6 LEDs to illuminate the fingernail and an array of 8 photodetectors to measure the coloration. The extremely sparse sample of the color patterns in the nail has limited the sensor to a low measurement ($2 - 3N$ (newton)) range and accuracy ($0.5 - 1N$ error).

To best locate the 8 photodetectors in the *photoplethysmograph sensor*, images of the 6 different fingertip force states for 16 human subjects have been studied in [7, 8]. At the point of contact, the force vector $F = [F_x F_y F_z]$ is defined such that F_z is the normal force, F_x is the lateral shear force, and F_y is the longitudinal shear force (positive direction forward). The six force states were: zero force = $[0 0 0]N$, normal force = $[0 0 -3]$, left shear = $[-2 0 -3]$, right shear = $[+2 0 -3]$, backward shear = $[0 -2 -3]$, and forward shear = $[0 2 -3]$. (To produce a shear force without slipping, subjects were asked to produce

3N of normal force.) By manually thresholding the images, normal force, negative and positive lateral shear force, and negative and positive longitudinal shear force, all result in visibly different patterns of coloration.

With a high resolution video camera to image the full back of the fingertip, our previous work [11, 12] have studied the color response in the fingernail and surrounding skin pixel by pixel. A detailed analysis of the static and dynamic color response of each pixel (0.04-by-0.04 mm area) in the fingernail was carried out for all regions of the fingernail and surrounding skin. We found that pixels in different regions of the fingernail and surrounding skin respond to the force differently [11]. Some areas respond well to all components of force, other areas are unique to a force component. The observed best regions were consistent with the observation in [7, 8].

A full study of the color pattern responding to the fingertip force is not only important for better design of fingernail force sensors, but also important to understand the sensing mechanism, including the mechanics of the fingernail-bone-tissue interaction and its effect on blood perfusion. The mechanism behind the hemodynamic response to normal force has been quantitatively modeled in [7], but the response to shear force requires further study.

Because of potential use in human-computer-interaction, researchers have tried to prove that different directional forces result in measurably different blood perfusion patterns that are common to all people. It has been showed in [9] that after cropping and normalization according to the length and width of the fingernail, by pixel by pixel correlation, all of the images (one image per force state per person was taken) from one force state correlated best to the average image of the true force state with better than 99% confidence, with the exception of normal force and backward shear force which had similar patterns of coloration. They concluded that the fingernail coloring patterns under various force conditions were statistically different for all people for 5 discrete forces (zero force, normal force, negative and positive lateral shear force, and positive longitudinal

shear force). These results provided a necessary condition to conclude that the fingernail color patterns corresponding to directional forces could be automatically recognized.

To have the sufficient condition of the conclusion, this paper devises a method based on Linear Discriminant Analysis (LDA) to extract linear features and use them to identify the color patterns in the fingernail and surrounding skin. The force level for each direction is no longer restricted as in [9]. Instead, subjects are instructed to apply arbitrary force levels as they prefer. The method is verified on 7 subjects with different levels of force.

To make a comparison between images, intrasubject and intersubject registrations are carried out. The intrasubject registration registers different frames of one finger to a reference frame. It includes a Harris feature detection and RANSAC homography registration. The intersubject registration registers images of different fingers to an atlas image for the convenience to obtain the common color patterns for all people. Instead of simply normalizing the width and height of the nails, we use an elastic model registration that warps the images of the fingernail and surrounding skin to the exact shape defined in an atlas to minimize the mismatching error.

2. Finger Image Registration

We assume the distal phalanx is a rigid body, which is true when the observation is the back of the distal phalanx and the small deformation of the side skin can be ignored. When the distance between the finger and the camera is far larger than the curvature of the fingernail, we can assume that the surface of the fingernail and surrounding skin is planar.

To study the color pattern in the fingernail and surrounding skin in response to different fingertip force directions requires an analysis of images taken at different times. Finger posture varies over time relative to the camera. To compare the images, it is necessary to align them to avoid the orientation and position difference. We call the registration between images of one finger as intrafinger registration.

To study the color pattern across the population, images of different fingers have to be comparable. Meaningful regions such as the distal, middle and proximal zone of the nail should be consistent for different fingers. We call the registration of different fingers to an atlas finger as interfinger registration.

2.1. IntraFinger Registration

Since we assume the surface of the fingernail and surrounding skin is a plane, the transformation between a point (x', y') in a new image and a point (x, y) in the reference image is a homography:

$$\begin{bmatrix} x' \\ y' \\ 1 \end{bmatrix} = \mathbf{H} \begin{bmatrix} x \\ y \\ 1 \end{bmatrix},$$

where \mathbf{H} is a 3×3 matrix. To determine the 9 element in \mathbf{H} , it requires at least 4 correspondences in both images. The correspondences are automatically obtained with feature detection [5], correlation, and RANSAC [3] as follows:

1. Use Harris feature point detection [5] to automatically detect feature points in both the new image (Figure 1 (A)) and the reference image (Figure 1 (B)), as shown in Figure 1 (C).

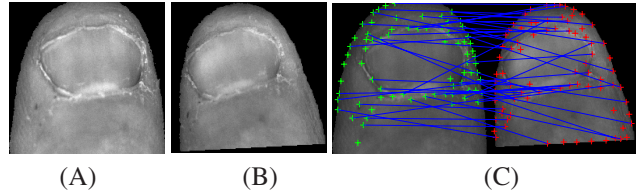


Figure 1. (A) The reference image. (B) A new image. (C) Feature points are marked as '+'s in both images. The corresponding pairs obtained with correlation are connected with lines.

2. Pair the detected feature points in two images by looking for points that are maximally correlated with each other within windows surrounding each point. Only points that correlate most strongly with each other are paired. Figure 1 (C) shows the pairing by connecting the corresponding points with lines.
3. Robustly fit a 2D homography mapping model with RANSAC to select inliers as shown in Figure 2 (A). The inliers are the correspondences.

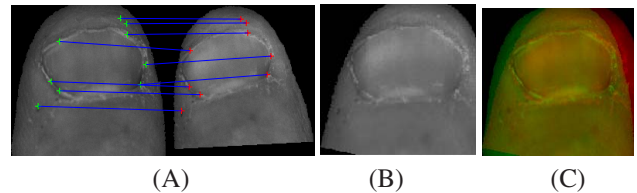


Figure 2. (A) The correspondences after RANSAC. (B) The intrafinger registration result. (C) Registration result (red) overlaps the reference image for comparison (green).

With the correspondences in the new image and the reference image, the 2D homography can be calculated with least squares. With the homography matrix, the new image is then mapped to the reference image. Figure 2(B) shows the transformation result. Figure 2(C) shows the overlap of the transformation result and the reference image. We can see that they match well. With the same process, each new image of a finger is mapped to the reference image.

2.2. InterFinger Registration

For the convenience of analysis, a regular shape atlas finger image is built as shown in Figure 3(F). The fingernail is modeled as a disk. The surrounding skin region is composed with a ring and an isosceles trapezoid. The exact size of each portion is illustrated.

To register the fingernail and surrounding skin, the fingernail in the reference images need to be segmented from the surrounding skin. We use a Canny edge filter to automatically detect the boundary of the fingernail. However, because of the broken skin around the fingernail, the automatically detected boundary is noisy. It rarely forms a smooth curve. The edge detection result of a typical finger (Figure 3(A)) is shown in Figure 3(B). We use cubic B-splines to fit the edges and achieve a close-loop contour as shown in Figure 3(C). The region inside of the contour is the segmented nail as shown in Figure 3(E).

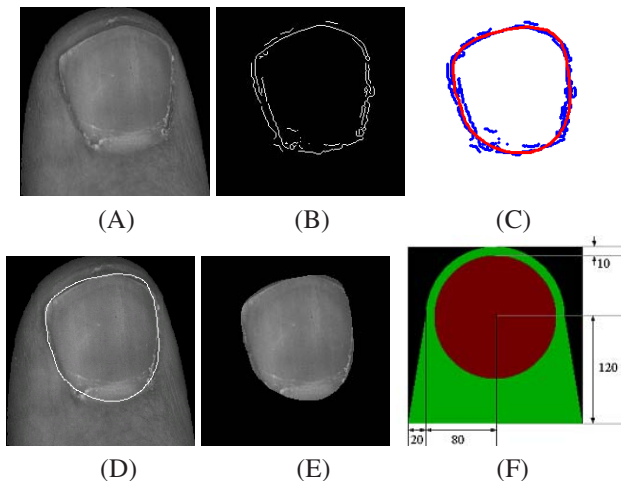


Figure 3. (A) The finger image. (B) Canny edge detection result. (C) Cubic B-spline fits the edges. (D) The contour of the fingernail is shown as a white closed-loop. (E) The region within the boundary is the fingernail. (F) The atlas of the full back of the fingertip. The fingernail is modeled as a disk with 70 pixels radius. The surrounding skin region is composed as a ring (70 pixels inner radius and 80 pixels outer radius), and an isosceles trapezoid (160 pixels and 200 pixels for two bases respectively).

The nail and the surrounding skin can be transformed to the atlas image respectively with boundary-based elastic deformation transformation [2, 10]. We model both the fingernail and surrounding skin regions as elastic sheets that are warped by an external force field applied to the boundaries. Since elastic warping tends to preserve color pattern shapes and the relative position of the patterns, it is well-suited for color pattern comparison across subjects.

We assume both the fingernail boundary and surrounding skin boundary can be homothetically transformed to the defined boundary in the atlas image. The boundaries in an

image are first deformed into their corresponding boundaries in the atlas. The mapping of the rest of the images is calculated by solving the equations describing the deformation of an elastic sheet with the boundary deformations. Detailed description can be found in [2, 10] with different elastic models. With the elastic deformation model, the pixel to pixel mapping can be calculated.

The interfinger registration process is illustrated in Figure 4. After the fingernail and surrounding skin are registered respectively (Figure 4 (1) and (2)), the registration results are combined together to generate the registration of the whole finger image (Figure 4 (3)).

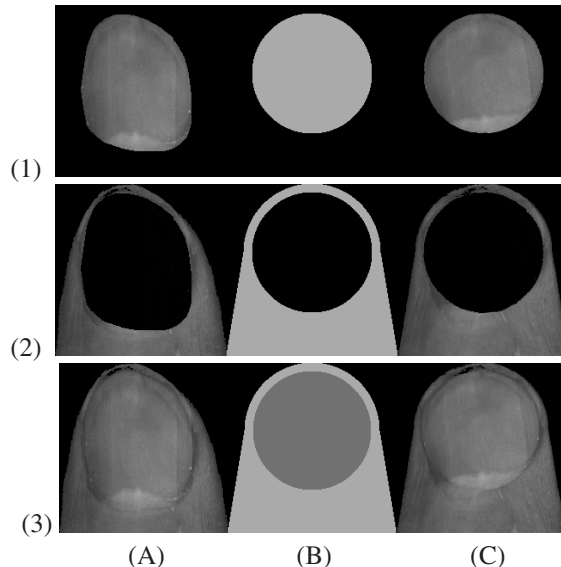


Figure 4. Column (A) (1) - (3) are segmented fingernail, surrounding skin, and the whole finger image. Column (B) (1) - (3) are atlases of fingernail, surrounding skin, and the whole finger. Column (C) (1) - (3) are interfinger registration results for fingernail, surrounding skin and two combined together.

The interfinger registration results for all the other 6 subjects are shown in Figure 5. The registration results preserve color pattern shapes and the relative position of the patterns.

3. Setup

With a 1024-by-768 color video camera (Flea camera from Point Grey Research), we collected 10 images for each of the 6 force directions for 7 subjects varying in age, size, sex and race. All the auto adjustment functions of the camera were turned off to make sure the internal condition of the camera does not change over images. A lighting dome as in [11] was used to provide a consistent uniform lighting condition.

In contrast to [9], subjects were allowed to apply different levels of shear and normal force according to their comfort. The subjects were given visual feedback about

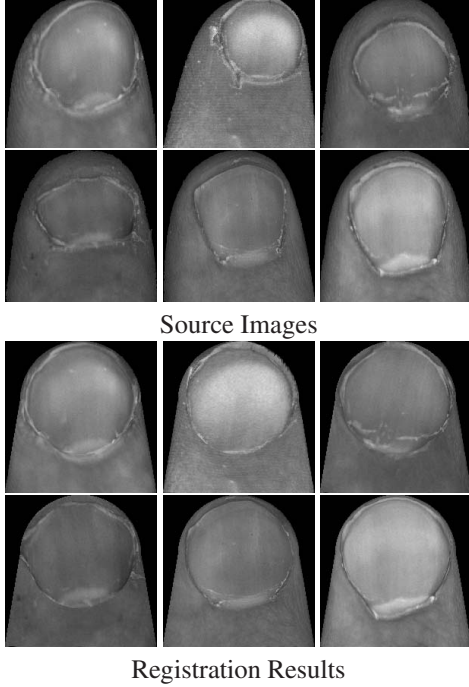


Figure 5. The elastic registration result for the other six subjects.

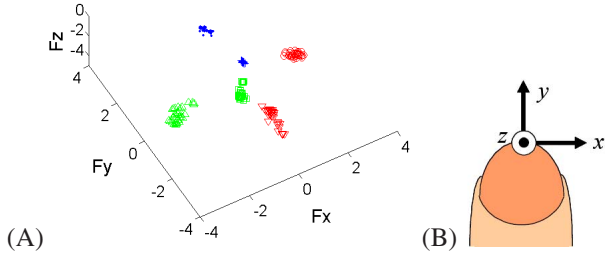


Figure 6. (A) The force levels for each force group ($+F_x$ (o's), $-F_x$ (Δ 's), $+F_y$ (·'s), $-F_y$ (∇), F_z (\square 's), and F_{zero} (+'s)); (B) The force directions relative to the fingertip

the magnitudes and directions of the fingertip force components using a graphical display as in [11], so that they could hold their chosen force levels. For directional shear forces, the subjects needed to exert some normal force to prevent sliding. For zero force, the subjects were asked to rest their fingers on the force sensor to yield a small normal force. An example for one subject is shown in Figure 6 (A). Subjects were asked to remove their fingers from the force sensor between recordings.

One zero-force image of each subject is selected to be the intrafinger reference image. All the other nail images for each subjects are registered to the reference images with intrafinger registration in section 2.1. All the intra-registered images of other subjects are registered to the atlas with intrafinger registration in section 2.2.

4. Color Pattern Identification with LDA Method

As discovered in [9, 11], with different directions of force applied on the fingertip, the color patterns in the fingernail and surrounding skin are different. The different color patterns can be used to classify the finger images to 6 classes corresponding to 6 force directions. Since the color patterns in the images are very high dimensional, we need a feature extraction method to find the features to best describe the color patterns. Considering that the application of this technique requires real-time, a linear feature extraction is preferred [6]. Moreover, because we are seeking common color pattern features for all people, the extracted feature should not only maximize the differences between the 6 classes, but also minimize the variation between subjects. The well-known linear discriminant analysis (LDA) [4, 1] is a good match.

The feature extraction problem is the same as to find projection vectors that maximize the ratio of the between-class scatter matrix \mathbf{S}_B to the within-class scatter matrix \mathbf{S}_W :

$$\mathbf{J}(\mathbf{W}) = \frac{|\mathbf{W}^T \mathbf{S}_B \mathbf{W}|}{|\mathbf{W}^T \mathbf{S}_W \mathbf{W}|} \quad (1)$$

It is the same as

$$\mathbf{J}'(\mathbf{W}) = \frac{|\mathbf{W}^T \mathbf{S}_B \mathbf{W}|}{|\mathbf{W}^T \mathbf{S}_T \mathbf{W}|} \quad (2)$$

where $\mathbf{S}_T = \mathbf{S}_W + \mathbf{S}_B$ is the scatter matrix of the whole data. Finding the vectors to maximize $\mathbf{J}'(\cdot)$ is a generalized eigen-problem. The columns of an optimal \mathbf{W} are the $C - 1$ generalized eigenvectors of

$$\mathbf{S}_B \mathbf{w}_i = \lambda_i \mathbf{S}_T \mathbf{w}_i, \quad (3)$$

where the C is the number of classes. Here $C = 6$. Since \mathbf{S}_T is always singular when the number of training data is smaller than the dimension of the data, a principle component analysis (PCA) is used to reduce the dimension [1]. This process is usually referred to as PCA-LDA. As studied in [13], the performance of the PCA-LDA approach heavily depends on the selections of principal components (PCs) in the PCA step. We use a PCA selection scheme based on the correlation between the PCs of \mathbf{S}_T and the PCs of \mathbf{S}_B [13].

4.1. Extraction of Linear Features

630 training images are taken for 6 force directions of 7 subjects. All images are resized to 50×50 and labeled. All images are registered to their reference image and then to the atlas. With LDA, the linear feature vectors are extracted and illustrated as in Figure 7. The pixel values of the pixels are the weights from feature vectors. The weights can be

positive or negative. The top row and bottom row in the Figure 7 shows the positive and negative weights respectively.

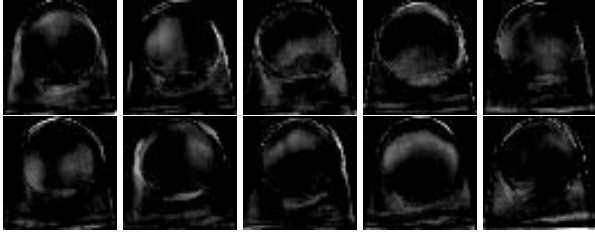


Figure 7. 5 linear discriminant features for 7 subjects. The features are shown in 2 rows. The top row shows the positive features and the bottom row shows the negative features.

The features in fingernail are isolated in Figure 8. The highlights in the distal and middle of the nail atlas (column 2, 3 and 4 from left in Figure 8) are consistent with previous observations: white zones observed in [7, 8, 9] and the best response regions in [11]. The feature regions in the column 4 have been explained as the interaction between tissue, nail and bone [7]. The other highlight regions are the left-distal, left-proximal, right-distal and right-proximal portions of the nail respectively. This is consistent with previous observations, but previously not much was done regarding this these particular observations. These results may also be valid for the mechanical study of the nail-bone-tissue interaction. Other than the nail, the surrounding skin also has useful feature regions.

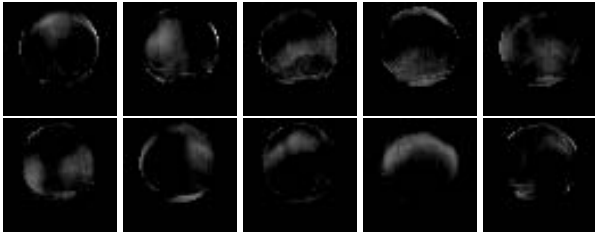


Figure 8. Features in the fingernail

The feature space is 5 dimensional. Figure 9 shows the training data in the 2 dimensional plane spanned with the first two Fisher feature vectors. We can see that even with just 2 feature vectors, images with $+F_x$, $-F_x$, $+F_y$ and $+F_{zero}$ are well separable.

4.2. Classification of New Images

Recognition is made in a 5 dimensional space spanned by the Fisher vectors. New images are projected to the Fisher feature space and classified based on the L_2 norm distances to the centroids of the 6 training clusters.

The recognition results for 790 new images of 6 force directions of 7 subjects are shown in Table 1, which contains

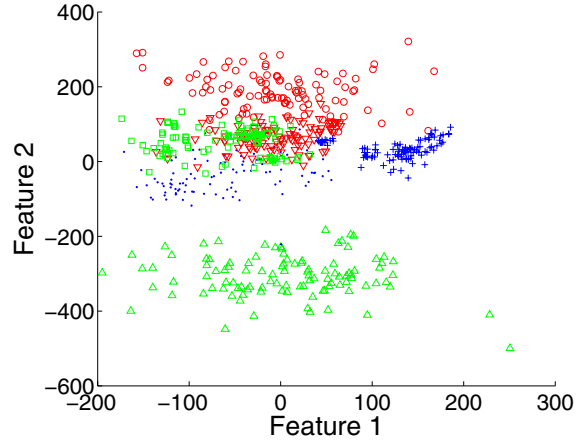


Figure 9. Training images are projected in the plane spanned with the first 2 feature vectors. Six clusters represent the lateral shear force directions $+F_x$ (\circ 's) and $-F_x$ (Δ 's), the longitudinal shear force directions $+F_y$ (\cdot 's) and $-F_y$ (∇), normal force F_z only (\square 's), and no force ($+$'s).

Index	All	No $-F_y$	Force	All	No $-F_y$
1	99%	100%	x	97%	96%
2	93%	97%	x-	98%	98%
3	93%	96%	y	98%	99%
4	94%	100%	y-	69%	—
5	89%	98%	z	94%	100%
6	87%	97%	zero	96%	100%
7	85%	100%	—	—	—
Total	92%	98%	Total	92%	98%

Table 1. The columns from the left to right are the subject index, the accuracy in percentage for each subject with 6 force directions in consideration, the accuracy in percentage for each subjects without considering $-F_y$, the force directions for all subjects, and the accuracies for all subjects categorized by force direction with and without $-F_y$.

2 subtables. The left one lists the subject index, accuracy of each subject considering all force directions, and accuracy without considering the $-F_y$ direction. The right one lists the force directions, accuracy of all subjects for each direction, and accuracy of all subjects for each direction without $-F_y$.

The overall accuracy of this method is 92% with $-F_y$ and 98% without it. For all force directions, the accuracies for all subjects are all over 85%. Four out of seven subjects have more than 90% accuracy. When looking into the accuracy for different force directions, the accuracies of all directions except $-F_y$ are equal to or more than 94%. The accuracy for recognizing $-F_y$ is relatively low. Around 80% of the misclassified $-F_y$ is misclassified to F_z . Not considering $-F_y$, the overall accuracy goes up to 98%.

5. Conclusion

The fingernail images of different people have been successfully registered to an atlas with elastic registration. 5 linear features of the color patterns corresponding to the directional force are extracted with LDA. The feature regions in the atlas are consistent with common observations and previous studies. The new discovered feature regions can be useful in the study of fingernail-bone-tissue interaction. The verification experiment validates that the color pattern identification method based on the linear features is fairly accurate and repeatable even when the force levels are not restricted.

The low accuracy of $-F_y$ indicates that the common color patterns of the longitudinal shear $-F_y$ is very close to the common color patterns of just normal force F_z , since most misclassifications went to F_z . The differences between the $-F_y$ and F_z color patterns are not significant enough to overcome the differences between subjects. However it is possible that by looking at features of each individual subjects, the differences of the color patterns between $-F_y$ and F_z might be significant. Except for this case, the proposed method provides a feasible and valid way to identify the force direction on the fingerpad remotely. We have shown for the first time that finger forces, not just finger position, can be measured with ordinary cameras. The technique alone or combined with finger tracking technique can provide a natural input method for human-computer interaction.

This method currently is limited to recognizing 6 color patterns due to orthogonal forces. We found that the color pattern in the fingernail and surrounding skin changes continuously with the changes of force direction on the fingertip. Since our method is base on linear feature extraction, the continuity property remains in the LDA feature space. In the future, we will further investigate the possibility of using the continuity property and Euclidean distances to centroids to continuously estimate the force direction. Further, we will investigate the possibility of integrating this technique with the force estimation in isolation in [11] to predict 3D force continuously.

Acknowledgments

This work was supported by NIH Grant 1R21EB004600-01A2.

References

- [1] P. N. Belhumeur, J. P. Hespanha, and D. J. Kriegman. Eigenfaces vs. fisherfaces: Recognition Using Class Specific Linear Projection. *IEEE Tran. on Pattern Analysis and Machine Intelligence*, 19(7):711-720, 1997.
- [2] C. A. Davatzikos, R. N. Bryan and J. L. Prince. Image registration based on boundary mapping. *IEEE Trans. Medical Imaging*, 15:112-115, 1996.
- [3] M.A. Fischler. and R.C. Bolles. Random sample consensus: A paradigm for model fitting with applications to image analysis and automated cartography. *Comm. Assoc. Comp. Mach.*, 24:381-395, 1981.
- [4] R. A. Fisher. The statistical utilization of multiple measurements. *Annals of Eugenics*, 8:376C386, 1938.
- [5] C.G. Harris and M.J. Stephens. A combined corner and edge detector. *Proc. Fourth Alvey Vision Conference*, 147-151, 1988.
- [6] A.M. Martinez and M. Zhu. Where Are Linear Feature Extraction Methods Applicable? *IEEE Transactions on Pattern Analysis and Machine Intelligence*, 27(12):1934-1944, 2005.
- [7] S.A. Mascaro and H. H. Asada. Photoplethysmograph Fingernail Sensors for Measuring Finger Forces without Haptic Obstruction. *IEEE Trans. Robotics and Automation*, 17: 698-708, 2001.
- [8] S.A. Mascaro and H.H. Asada. Measurement of Finger Posture and Three-axis Fingertip Touch Force Using Fingernail Sensors. *IEEE Trans. Robotics and Automation*, 20: 26-35, 2004.
- [9] S.A. Mascaro and H.H. Asada. The Common Patterns of Blood Perfusion in the Fingernail Bed Subject to Fingertip Touch Force and Finger Posture. *Haptics-e*, 4(3):1-6, 2006.
- [10] S. Periaswamy. and H. Farid. Elastic registration in the presence of intensity variations. *IEEE Trans. Medical Imaging*, 22, 865-874, 2003.
- [11] Y. Sun, J.M. Hollerbach, and S.A. Mascaro. Measuring Fingertip Forces by Imaging the Fingernail. *Proc 14th Symposium on Haptic Interfaces for Virtual Environment and Teleoperator Systems*, 125-131, 2006.
- [12] Y. Sun, J.M. Hollerbach, and S.A. Mascaro. Dynamic Features and Prediction Model for Imaging the Fingernail to Measure Fingertip Forces. *ICRA06*, 2813-2818, 2006.
- [13] M. Zhu and A.M. Martinez. Selecting Principal Components in a Two-Stage LDA Algorithm. *CVPR06*, 1:132-137, 2006.